applied microbiology

MDPI

Article

Genome Comparison of '*Candidatus* Phytoplasma rubi' with Genomes of Other 16SrV Phytoplasmas Highlights Special Group Features

Jan Werner Böhm [1], Dominik Duckeck [1], Bojan Duduk [2], Bernd Schneider [3] and Michael Kube [1,*]

[1] Department of Integrative Infection Biology Crops-Livestock, University of Hohenheim, 70599 Stuttgart, Germany; jan.boehm@uni-hohenheim.de (J.W.B.); dominik.duckeck@uni-hohenheim.de (D.D.)
[2] Institute of Pesticides and Environmental Protection, 11080 Belgrade, Serbia; bojan.duduk@pesting.org.rs
[3] Institute for Plant Protection in Fruit Crops and Viticulture, Julius Kühn-Institut, Federal Research Centre for Cultivated Plants, 69221 Dossenheim, Germany; bernd.schneider@julius-kuehn.de
* Correspondence: michael.kube@uni-hohenheim.de; Tel.: +49-(0)711-459-24910

Abstract: Phytoplasmas are associated with important bacterial diseases, causing severe symptoms in agricultural and ornamental crops. '*Candidatus* Phytoplasma rubi', associated with the *Rubus* stunt in raspberries (*Rubus idaeus*) and blackberries (*Rubus* subgenus *Rubus*), causes shortened internodes, elongated sepals, proliferation, phyllody, and virescence. The recently published genome of '*Ca.* P. rubi' RS enabled a comprehensive genomic comparison to the complete genomes of 16SrV phytoplasmas, comprising strains of the flavescence dorée-associated phytoplasma CH and two '*Candidatus* Phytoplasma ziziphi' strains. Besides the typical transporters and metabolic features of phytoplasmas, the phosphorolysis of sucrose and the utilization of the carboxylic acid L-lactate became apparent for the 16SrV-group. With respect to the effector repertoire and the encoded immunodominant membrane proteins involved in host colonization, the group revealed conserved features that comprise the variable membrane proteins A and B. However, SAP11- and SAP54 orthologs were limited to '*Ca.* P. rubi' RS and '*Ca.* P. ziziphi'. Genome-sequence-based phylogenetic analysis supports the close relationship of these genomes relative to alder yellows phytoplasmas. The analyses supported the impact of the mobilome on phytoplasma evolution but also highlighted that there is the possibility of identifying phytoplasmas with a larger metabolic repertoire in the future.

Keywords: *elm yellows phytoplasmas*; *Rubus* stunt; flavescence dorée; metabolism; effector repertoire

Citation: Böhm, J.W.; Duckeck, D.; Duduk, B.; Schneider, B.; Kube, M. Genome Comparison of '*Candidatus* Phytoplasma rubi' with Genomes of Other 16SrV Phytoplasmas Highlights Special Group Features. *Appl. Microbiol.* **2023**, *3*, 1083–1100. https://doi.org/10.3390/applmicrobiol3030075

Academic Editor: Ian Connerton

Received: 3 August 2023
Revised: 7 September 2023
Accepted: 9 September 2023
Published: 12 September 2023

1. Introduction

Phytoplasmas are insect-transmitted, cell-wall-less bacteria in the Mollicutes class colonizing plants and insects [1]. The specific characteristics of phytoplasmas led to a classification of these organisms in the provisional taxon '*Candidatus* Phytoplasma' [2]. Among others, the 16S rRNA gene was the predominant genetic marker for this taxon [3], and restriction fragment length polymorphism analyses of the 16S rRNA gene were applied to distinguish and classify different phytoplasma taxa [4]. One of these ribosomal groups is the 16SrV group [5,6], which is synonymously named *elm yellows phytoplasmas*, comprising strains of '*Candidatus* Phytoplasma ulmi', '*Candidatus* Phytoplasma rubi', alder yellows phytoplasma, and '*Candidatus* Phytoplasma ziziphi', which are associated with diseases in genera such as *Ulmus*, *Rubus*, *Alnus*, *Vitis*, and *Ziziphus* [6–9]. Herein, the *Rubus* stunt disease of blackberries (*Rubus* subgenus *Rubus*) and raspberries (*Rubus idaeus*) is associated with '*Ca.* P. rubi' and different cultivars display typical symptoms such as stunting, elongated sepals, phyllody, proliferation, and virescence [10–12]. Abnormal growth and poor fruit quality and quantity result in high economical losses [13]. These problems are also well known for flavescence dorée (FD), a serious threat to European viticulture associated with

the FD phytoplasmas, which cause plant decline, changes in leaf habitus and colour, and subsequent reduction in grape quantity and quality [14]. The 16SrV group phytoplasmas '*Ca.* P. ulmi' and '*Ca.* P. ziziphi', which infect deciduous tree species in North America, Europe, and Asia, are associated with shoot proliferation known as witches' brooms [15,16]. However, in Europe, infections of elms and alder (*Alnus glutinosa* L.) by '*Ca.* P. ulmi' and the *alder yellows* phytoplasmas, respectively, are common but symptom formation is rare [15,17], indicating the existence of tolerance in these hosts.

The recently increasing number of phytoplasma genomes has enabled genome-wide comparisons applied for the genomic relationship of phytoplasma species that have become more apparent in recent years [3,18]. Classification of phytoplasmas by bioassays is not yet possible due to the lack of established in vitro cultures, which limits the metabolic characterisation of these bacteria to the genomic level, highlighting the importance of genomic comparisons. These parasitic bacteria are dependent on their hosts for their entire life cycle and are restricted to a limited number of nutrient-rich environments [19,20]. Specialisation in these narrow environments has led to high levels of reductive evolution. Their genomes are subject to evolutionary condensation, resulting in sizes between 530 kb and 930 kb defining the genomic content for sustenance in different hosts and for adaption to a certain range of environments [21,22]. In contrast to the closely related *Acholeplasma* spp., phytoplasmas encode only a small fraction of enzymes involved in metabolic pathways such as glycolysis, pyruvate degradation, and glycerophospholipid metabolism [23,24]. Cell membrane translocation proteins such as ABC transporters, ATPases, and symporters are essential for survival in these special environments, allowing the influx and efflux of various substrates including carbohydrates [25], cations [26], and acids [27], making them essential for glycolysis, carboxylic acid metabolism, acetogenesis, glycerophospholipid metabolism, and ion pool regulation [26,28].

After the release of the "flavescence dorée" phytoplasma genome [29] and two '*Ca.* P. ziziphi' genomes [30,31], we have recently published the genome sequence of '*Ca.* P. rubi' RS [32], resulting in four complete genomes of 16SrV phytoplasmas. Here, we provide a comparative genome analysis of those four 16SrV phytoplasmas, highlighting peculiarities in host-dependent metabolism and secretome.

2. Materials and Methods

2.1. Genome Data Curation

Data analysis including a cumulative GC-skew analysis of the complete genome sequences of '*Ca.* P. rubi' RS (updated acc. no. CP114006.1), '*Ca.* P. vitis' CH (acc. no. CP097583.1), '*Ca.* P. ziziphi' Jwb-nky (acc. no. CP025121.1), and '*Ca.* P. ziziphi' Hebei-2018 (acc. no. NZ_CP091835.1) was performed using Artemis Genome Browser v. 18.1.0 [33]. In addition, an automatic annotation pipeline for comparisons that excluded differences in genomes due to annotation styles was performed using Rapid Annotation Subsystem Technology v. 2.0 (RAST) [34]. The inspection of annotated coding sequences was carried out using the information provided by the database and the basic local alignment search tool (BLAST) [35]; moreover, the nonredundant protein database of the National Center for Biotechnology Information (GenBank release 255.0) [36] was used as the subject, and the protein content of four phytoplasma genomes was deduced as the query.

2.2. Metabolic Reconstruction

Metabolic reconstruction was performed using software packages Metacyc v. 27.0 [37], KEGG v. 105.0 [38], and InterProScan v. 93.0 [39]. The prediction of amino acid sequences carrying transmembrane regions and/or signal peptides in the '*Ca.* P. rubi', '*Ca.* P. vitis', and '*Ca.* P. ziziphi'-deduced proteins was performed using Phobius v. 1.01 [40], resulting in three groups of peptide sequences that carry transmembrane helices and/or signal signatures. Comparative genome analysis with Orthologous MAtrix (OMA) v. 2.5.0 and OrthoFinder v. 2.5.4 [41,42] was performed on the deduced protein content with respect to

orthology inference. Hypothetical proteins were included throughout the analysis. Venn diagrams were constructed using InteractiVenn [43].

2.3. Phylogenetic Analysis

The phylogenetic analysis of the deduced L-lactate amino acid sequence was performed using the Molecular Evolutionary Genetics Analysis (MEGA) v. 10.1.7 [44] software package and the MUSCLE algorithm for amino acid alignments with default settings; moreover, the maximum likelihood method was used for phylogenetic analyses, with 1000 replications carried out and the default settings applied. The sequences of L-lactate dehydrogenase (LdH) for the phylogenetic analysis of species belonging to *Acholeplasmataceae* were derived from GenBank (release 255.0) by carrying out BLASTP searches relative to the non-redundant protein sequence database that is limited to *Acholeplasmataceae* using the LdH amino acid sequence of '*Ca.* P. rubi' RS (RS_02750, Table S1) as query; moreover, the subject sequences were obtained with an e-value cut-off at 2×10^{-11}. Subject sequences covering less than 70% of the query sequence were removed. The LdH amino acid sequence of *Anaeroplasma bactoclasticum* was added and used as an outgroup to root the tree. For average nucleotide identity analyses, QIAGEN CLC Genomics Workbench v. 21.0.5 (QIAGEN, Aarhus, Denmark, https://digitalinsights.qiagen.com (accessed on 16 May 2023)) and the included whole-genome alignment tools were used with standard options except for the seed length of 13 in the initial alignment options; moreover, the phylogenetic tree was constructed based on the neighbour-joining method.

3. Results and Discussion

3.1. Genomic Benchmarks

The comparison of total coding sequences (CDS), coding density, and average CDS length was enabled using the annotation pipeline (RAST) (Table 1). The highest amount of CDS was observed for RS (887), followed by Hebei-2018 (787), Jwb-nky (719), and CH (534), and they were observed in the same order with respect to coding densities in CDS as follows: kb 1.163, 1.029, 0.957, and 0.816, respectively. This first glance already shows the special position of the FD-associated strain CH. All four phytoplasma species share a common number of rRNA operons (2) and tRNAs (33 in Hebei-2018, resulting from a double), which is in line with the typical benchmarks of phytoplasmas [20]. Furthermore, a G + C content below 24% can be observed in all four chromosomes. The lowest G + C content and sequence length are obtained for the chromosome of the CH strain, while the RS strain has a >108 kb larger chromosome with a 1.79% higher G + C content. Extrachromosomal elements have not been identified in the 16SrV phytoplasmas studied [29–32].

Chromosomes show a circular organisation, supporting the hypothesis that linear chromosomes might be limited to the phylogenetic branch of the apple proliferation group [28]. Phytoplasma genomes are subject to rearrangements; therefore, they often comprise irregular cumulative GC skews [20], which is the case for all four studied genomes (Figure 1). Nevertheless, *dnaA* was found in proximity to putative *oriC* for '*Ca.* P. ziziphi' strains and was found in upstream areas for the CH and RS strains (Figure 1).

A repeated sequence of 11 kb was detected within the genome of the RS strain (position 158,785 to 170,488 and 356,223 to 367,894), which is partially encoded in the Jwb-nky strain (position 280,931 to 286,301 and 410,927 to 416,297) and Hebei-2018 (position 103,300 to 111,244 and 406,516 to 414,457), but not in CH (Figure 2). The coding repertoire of repeat one of RS is characterised by a transposase (*tra5*) and enzymes associated with DNA replication (DNA primase and DNA helicase) (Figure 2), which are associated with potential mobile units (PMUs). Moreover, the repeat one of RS shares ~3700 bp (161,273 to 164,951) with 88% identity with PMU2 of '*Ca.* P. asteris' AY-WB [45]. Based on the PMU-associated genes encoded in the 11 kb repeat of RS, this repeat has the characteristics of a PMU. PMUs are unique to phytoplasmas and have been observed in different phytoplasma species [45,46], contributing to genome plasticity [47].

Table 1. Overview of four complete phytoplasma 16SrV genomes.

Strain	'*Candidatus* Phytoplasma' Species rubi RS	ziziphi Jwb-nky	ziziphi Hebei-2018	*Vitis* CH
Chromosome organisation	Circular	Circular	Circular	Circular
Chromosome size [bp]	762,251	750,803	764,108	654,223
G + C content [%]	23.53	23.22	23.22	21.74
CDS	887	671	710	508
CDS coding	685	640	659	498
Hypothetical proteins	242	308	256	138
rRNA operons	2	2	2	2
tRNAs	32	32	33	32
Plasmids	0	0	0	0
Data source	CP114006.1 [32]	CP025121.1 [30]	NZ_CP091835.1 [31]	CP097583.1 [29]
	Data generated with automatic annotation pipeline (RAST)			
Coding density [CDS/kb]	1.163	0.957	1.029	0.816
average CDS length	655	824	730	944
CDS (RAST)	887	719	787	534

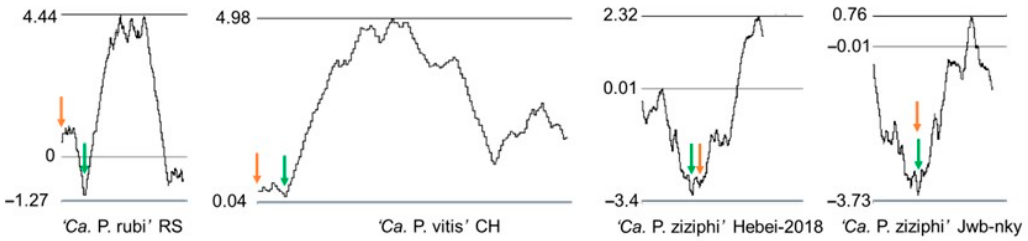

Figure 1. Cumulative GC skew ((G − C)/(G + C)) calculated with a window size of 5000 for the complete 16SrV chromosomes. Arrows indicate the location of *dnaA* (orange) and cumulative GC skew minimum (green) in the respective genome.

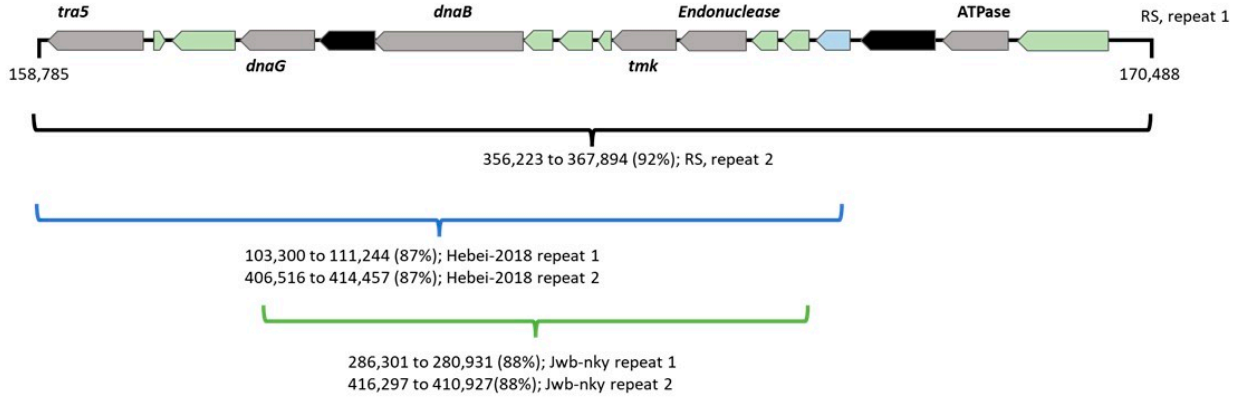

Figure 2. Repeat one of strain RS with annotated products (grey, as stated), green (hypothetical proteins), black (pseudogenes), blue (sequence variable mosaic (SVM) domain containing protein), in comparison to repeat two of RS (black parenthesis) and repeats of Hebei-2018 (blue parenthesis) and Jwb-nky (green parenthesis). The locations of each repeat are stated in bp with respect to circular organization of the chromosomes. Identities of each repeat compared to repeat one of RS are given in percentage in parentheses. Gene abbreviations: DNA primase (*dnaG*); DNA helicase (*dnaB*) and thymidylate kinase (*tmk*).

3.2. Pan-Genome Analysis

Pan-genome analysis enables the comparison of shared and unique features for the 16SrV group. In total, 16SrV phytoplasmas share a core number of 345 orthogroups (Figure 3) with assigned CDS and paralogs. The unique content of 16SrV phytoplasmas amount to 15% in orthogroups for the RS strain, 9% for CH, 4% for the Jwb-nky strain, and 9% for the Hebei-2018 strain. The unique orthogroups comprising CDS within '*Ca.* P. rubi' RS strain are not associated with assigned metabolic functions. Moreover, genes associated with PMUs, paralogs, and encoded hypothetical proteins contribute to the unique content of the RS strain. This observation in the 16SrV group is in line with other phytoplasmas that are characterised by reductive evolution, decreasing the genome's content and size on the one hand and, on the other hand, blowing up the genome due to the mobilome [20]. In the case of '*Ca.* P. rubi', an increased chromosome length is associated with a high prevalence of pseudogenes (202), and is in contrast to the chromosomes of the FD-associated CH strain (10) and the '*Ca.* P. ziziphi' Hebei-2018 (51) and Jwb-nky strains (31).

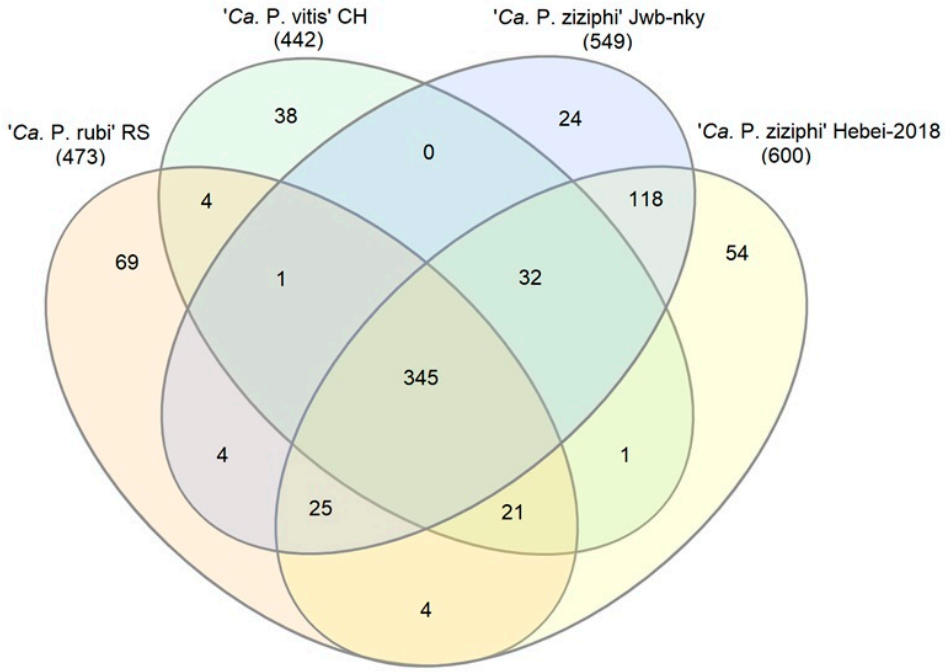

Figure 3. Orthogroups of the four 16SrV phytoplasma genomes. Colours have been assigned to the RS (orange), CH (green), Jwb-nky (blue), and Hebei-2018 (yellow) strains. The total number of the orthogroups of each genome is displayed in brackets.

3.3. Membrane Transport Proteins

ABC transporters that are encoded for carbohydrates (MalGFKE), spermidine/putrescin (PotABCD), methionine (MetINQ), and cofactors $Mn^{2+}/Zn^{2+}/Fe^{2+}$ (TroABCD) are conserved in the 16SrV genomes (Figure 4) and other phytoplasmas [20], suggesting a high dependency on these substrates. Sucrose and trehalose are major components in plant phloem and insect haemolymph [48–50], and the encoded ABC transporter MalGFKE is described to mediate the transport of these components [25]. Maltose is one of the main sugars transported in plants during starch breakdown at night [51]; therefore, it is another possible carbohydrate source for phytoplasmas in plants. Nevertheless, the exact carbohydrate template for imports and further processing in glycolysis remains unclear; thus, an unspecific import of carbohydrates is likely [20].

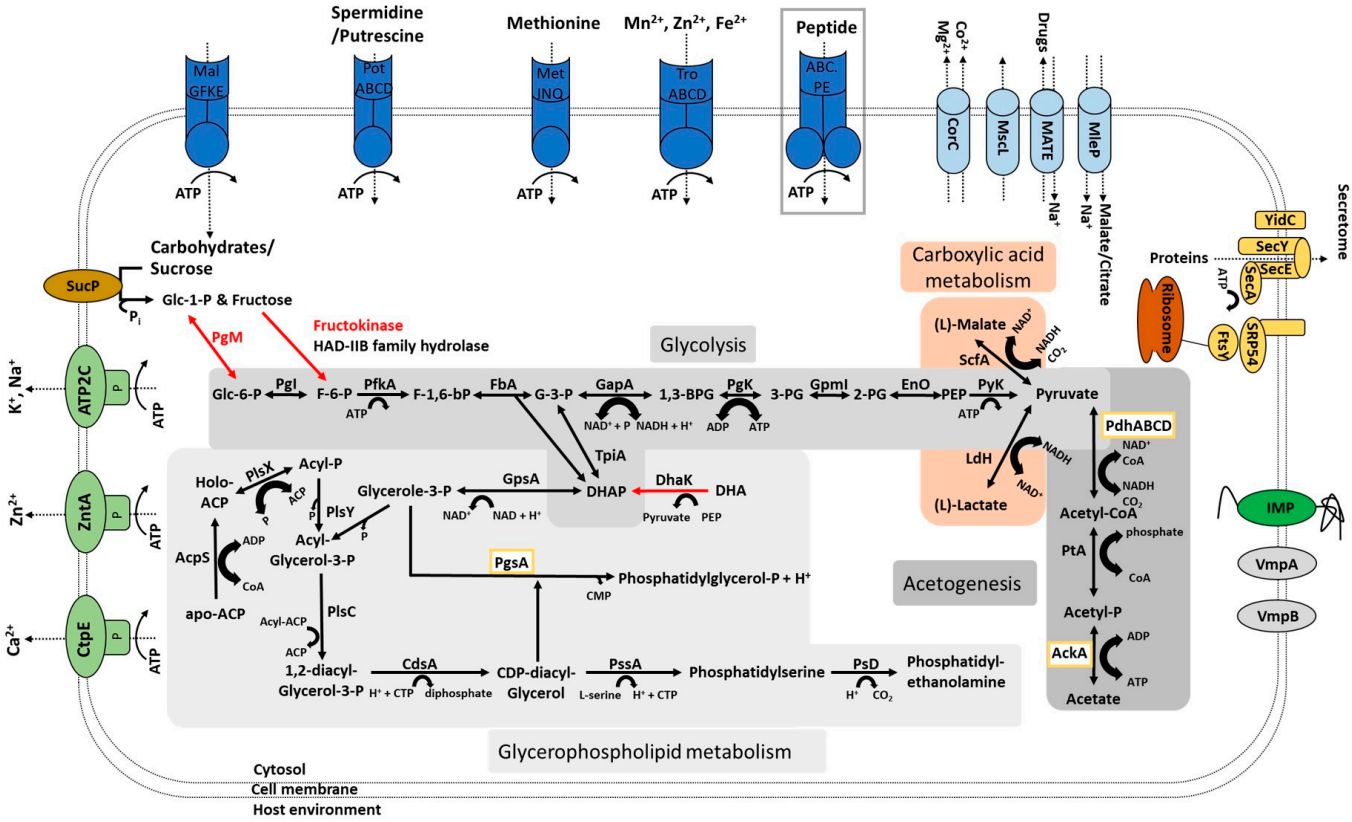

Figure 4. Predicted elements involved in transports at the membranes (P-type ATPases (green), ABC transporters (dark blue), Sec-dependent secretion system (yellow), transport proteins (light blue), and sucrose phosphorylase (brown) with respective substrates) in '*Ca.* P. rubi' RS, '*Ca.* P. vitis' CH, and in '*Ca.* P. ziziphi' Jwb-nky and Hebei-2018 strains. Transporters marked in the grey frame are limited to the genomes of '*Ca.* P. ziziphi' Jwb-nky and Hebei-2018. The predicted proteins in the studied genomes that are involved in glycolysis, acetogenesis, carboxylic acid metabolism, and glycerophospholipid metabolism are listed with their substrates, cofactors, and products. Straight arrows between the products indicate possible directions of enzyme catalysation, whereas curved arrows indicate the conversion of cofactors. Enzymes marked in red are not or only partially encoded in the studied genomes. Orthologous sequences for enzymes marked in yellow boxes are predicted in the genome sequences of '*Ca.* P. rubi' RS, '*Ca.* P. vitis' CH, and '*Ca.* P. ziziphi' Hebei-2018 but not in '*Ca.* P. ziziphi' Jwb-nky. Abbreviations for the depicted proteins are stated in the Results and Discussion section of this study.

The ABC transporter for the amino acid methionine is the only one predicted to mediate amino acid transport through the membrane for all four studied genomes. Besides the encoding of the substrate binding unit for peptides and nickel (ABC.PE) in '*Ca.* P. ziziphi', this transport mechanism seems to be conserved in the different phytoplasma strains of '*Ca.* P. asteris' and '*Ca.* P. mali' [20], raising questions about the putative peptide transport mechanisms for RS and CH strains.

Another shared feature within the 16SrV group is the three ion-pool-regulating P-type ATPases. These transporters mediate the export of K^+/Na^+ (ATP2C), Cd^{2+}/Zn^{2+} (ZntA), and Ca^{2+} (CtpE) with their respective PTHR43294, PTHR43079, and PTHR42861 protein domains. Although P-type ATPases are mainly described and found in monomeric states such as ZntA or CtpE, a dimeric structure was described for bacterial ATPases [52]. ATP2C contains the alpha subunit involved in translocation processes, whereas the second beta subunit component is suggested to mediate a chaperone and ATP hydrolysis function. With the alpha subunit solely encoded, which is also observed in *Acholeplasma* spp. and *Clostridium* spp. (according to PTHR43294), the translocation process of K^+/Na^+ is suspected to

be roughly functional due to the fact that this gene is part of the core genome of 16SrV phytoplasmas (Table S1).

The Na^+-driven export of drugs is mediated by the multidrug efflux channel (MATE), which is predicted for all four studied genomes. In response to mechanical stress such as stretch forces, a large conductance mechanosensitive channel (MscL) translates physical and osmotic forces [53] and is predicted for all studied phytoplasmas. A third transport protein is encoded and annotated as CorC, which mediates Co^{2+} and Mg^{2+} export through the cytoplasmic membrane.

The four genomes share a 2-hydroxycarboxylate transporter family protein (MleP). This conserved transporter enables the symport of malate/Na^+ and malate/citrate or the antiport of malate/lactate [27]. The symport function was suggested with respect to the utilisation of malate by the pyruvate acetate pathway in phytoplasmas [20,54]. One may speculate whether this enzyme in 16SrV phytoplasmas may also fulfil a malate/lactate antiporter function associated with malolactic fermentation, which yields energy based on membrane potential built up through lactate export and malate import [55]. This would contribute to the membrane potential utilised by F_OF_1-ATPases in relation to *Mycoplasma* spp. And *Acholeplasma* spp., but not in phytoplasmas that lack this system [23,56]. Nevertheless, the antiport function of MleP may contribute to lactate regulation in phytoplasma cells. The *mleP* gene was proven to be expressed in phytoplasmas [54], and a coupled import of malate with Na^+ allows for the further processing of malate to pyruvate, thereby accessing an energy-yielding pathway [20].

Transporters (Table S1) that are partially encoded or missing a substrate-binding unit are biotin transporter (EcfA/T), drug efflux transporter (EfrA/B), and unspecific ATP-binding proteins. Incomplete ABC transporters might be completed by the subunits of other transporters with respect to the shared repertoire, as suggested by Kube et al. 2012 [20], and thereby function in previously described transport processes.

3.4. Carbohydrate Metabolism

3.4.1. Sucrose Degradation

A striking feature of 16SrV phytoplasmas is the coding of a complete sucrose phosphorylase (Figure 4, SucP), enabling an efficient phosphorolytic cleavage of sucrose and P_i into D-fructose and alpha-D-glucose 1-phosphate [57]. The deduced protein sequence is anchored in the membrane by its unusual organisation with respect to the non-cytosolic and cytosolic domains separated by a transmembrane domain, suggesting transports across the membrane and ATP-independent phosphorylation [58]. Nevertheless, the necessary phosphoglucomutase enzyme (Figure 4, PgM) and a fructokinase for the further conversion of fructose and glucose 1-phosphate are not predicted in the studied genomes. Although these enzymes are missing, an unspecified haloacid dehalogenase superfamily subfamily IIb-containing enzyme was predicted in the four genomes. The enzymes of this family are predicted to bind substrates that are common in phytoplasma environments, such as glucose 6-phosphate, trehalose-6-phosphate, and fructose 6-phosphate, and they act as phosphatases or phosphotransferases [59]. With phosphatase activities, the use of trehalose 6-phosphate might be enabled [20], and phosphotransferase activity might facilitate the conversion of fructose to fructose-6-phosphate and thereby enable the latter to be used in the upper part of glycolysis (Figure 4).

3.4.2. Glycolysis

Glycolysis is a key energy-yielding metabolic process described for many phytoplasmas [24,29–31] and especially for 16SrV phytoplasmas in addition to the conserved malate–acetate pathway. In total, the four phytoplasmas share a conserved amount of nine encoded proteins involved in the glycolytic pathway (Figure 4), namely glucose-6-phosphate isomerase (PgI), 6-phosphofructokinase (PfkA), fructose-bisphosphate aldolase (FbA), glyceraldehyde 3-phosphate dehydrogenase (GapA), phosphoglycerate kinase (PgK), 2,3-bisphosphoglycerate-independent phosphoglycerate mutase (GpmI), enolase (EnO),

pyruvate kinase (PyK), and triosephosphate isomerase (TpiA), thereby encoding the enzymes for complete glycolysis from glucose 6-phosphate to pyruvate. This is in contrast to '*Ca.* P. mali', where necessary enzymes for glycolysis are only partially encoded, and as a result, alternative energy-yielding pathways are used [28]. It is also reported that crucial genomic content is missing in the peanut witches' broom (PnWB) phytoplasma genome, but the sequence is partial; therefore, it is not clear if unassembled regions may contain this genetic information [60].

3.4.3. Carboxylic Acid Metabolism

Phytoplasmas such as '*Ca.* P. mali' lack the crucial proteins of glycolysis and subsequently rely on alternative energy-yielding pathways by using carboxylic acids as energy sources [28]. In contrast to other phytoplasmas, 16SrV members encode two key metabolic enzymes (Figure 4): the NAD-dependent malic enzyme (ScfA) and the L-lactate dehydrogenase (LdH). These enzymes enable the reversible conversion of L-malate to pyruvate and subsequently to L-lactate [61,62]. Malate imports via the described MleP symporter ensure the presence of the substrate necessary for ScfA following conversion to pyruvate. Pyruvate is subsequently used as a substrate for LdH, resulting in lactic acid production. The reversible conversion of weak lactic acid can be used as a tool that mediates pH levels and osmotic stress due to the simultaneous conversion of NAD^+ and $NADH + H^+$. Lactate dehydrogenase is suggested to be subject to allosteric inhibition by malate, providing a method for overcoming lethal lactate concentrations in the cytosol [63]. Thus, favouring pyruvate that either comes from glycolysis or the oxidation of malate that is decarboxylated to acetyl-CoA enables the energy-yielding metabolism, as described for phytoplasmas, e.g., '*Ca.* P. mali' and PnWB phytoplasma [28,60].

One may speculate that L-lactate can be imported and used for pyruvate conversion because LdH is described to act reversibly in *Acholeplasma laidlawii* [64], but so far, no lactate-importing protein was described for phytoplasmas, thereby putting into question the substrate's abundance in phytoplasmas. The transport rate of lactate from the root to the tip of seedlings increased in hypoxic environments (below 7% O_2) while it decreased for malate and vice versa for oxic environments [50]. Furthermore, higher plants are able to build tissue niches with hypoxic conditions, even in aerobic environments that can be as low as 5% in potato tubers and 7% in the vascular system, especially in the phloem [65]. The change in weak acids in the plant habitat of phytoplasmas could be overcome by switching between malate and lactate as an energy source depending on availability, which is consistent with the stable phytoplasma abundance observed in *Oenothera* during changing atmospheric O_2/CO_2 levels [66].

A phylogenetic tree based on the deduced LdH amino acid sequence (Figure 5) corroborates the unique position of the 16SrV phytoplasmas in a monophyletic relationship with *Acholeplasma hippikon*, *Acholeplasma equirhinis*, and *Acholeplasma equifetale*, which is distinguishable from another LdH-cluster within *Acholeplasmataceae* comprising *Haploplasma modicum*, *Haploplasma axanthum*, *Mariniplasma anaerobium*, *Acholeplasma laidlawii*, and unspecified *Acholeplasma* species. The *ldh* gene is a distinctive genomic feature observed in 16SrV phytoplasmas, which is shared with the closely related *Acholeplasma* species. '*Ca.* P.' sp. AldY-WA1 (Figure 5) occurs as an unclassified phytoplasma species within the 16SrV cluster observed in phylogenetic analyses [67]; thereby, due to phylogeny and the occurrence of the *ldh* sequence, the grouping within the 16SrV can be supported.

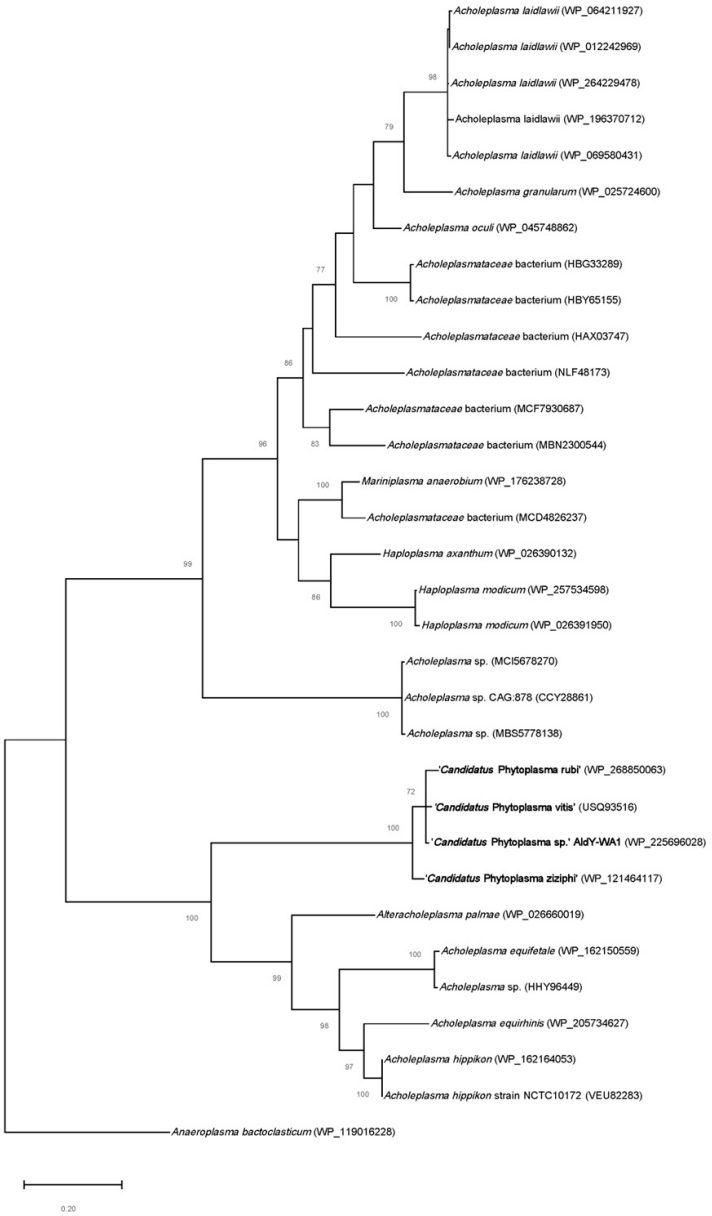

Figure 5. Phylogenetic tree for 32 L-lactate dehydrogenase (LdH) protein sequences of species belonging to *Acholeplasmataceae* and *Anaeroplasma bactocalsticum* as the outgroup. Bootstrap values above 70% are indicated. Accession number and strain information are displayed if available. The 16SrV phytoplasmas are highlighted in bold. The tree is derived to scale with the scale bar indicating 0.2 amino acid changes.

The genomic context of *ldh* in RS, CH, Jwb-nky, and Hebei-2018 (Figure 6) strains contain triosephosphate isomerase (*tpiA*), ATP-dependent DNA helicase (*uvrD*), and a xenobiotic response element family transcriptional regulator (*xre*). Triosephosphate isomerase is associated with *ldh* via their metabolic relationship in the glycolysis and genomic context within 16SrV chromosomes. Since lactate dehydrogenase has not yet been described for other phytoplasma species compared to phytoplasmas belonging to the 16SrV group [31], a question may be raised regarding whether *ldh* originated from a horizontal gene transfer. Such an option seems unlikely in view of the lack of coding for the phytoplasma typical transposons (potential mobile units, PMUs) in the Ldh-encoding acholeplasmas. The proximity to genes encoding FtsH and AAA+ ATPase, which are frequently associated with PMUs in '*Ca.* P. ziziphi' Jwb-nky [30,68], suggests that *ldh* has not escaped reductive

evolution in other phytoplasma branches. Further analysis on the origin of the 16SrV-*ldh* genes beyond the Acholeplasmatales indicates a Gram-positive origin [23].

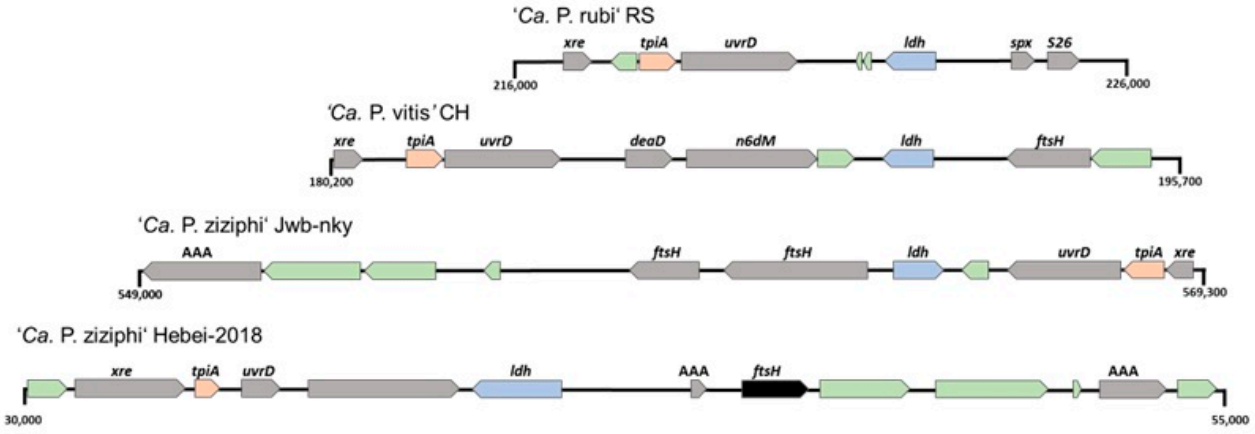

Figure 6. Genomic context of the L-lactate dehydrogenase gene (*ldh*, blue) for four phytoplasma strains. Gene names are indicated above the respective location, and orientation is indicated by an arrow. Chromosome location in base pairs is shown on the left and right of the respective region. Hypothetical proteins are displayed in green, coding regions are displayed in grey, pseudogenes are displayed in black, and genes encoding enzymes that are associated with LdH are displayed in light red. Gene abbreviations: Transcriptional regulator (*xre*); triose-phosphate isomerase (*tpiA*); ATP-dependent DNA helicase (*uvrD*); RNA-polymerase-binding regulatory protein (spx); S26 family signal peptidase (S26); box helicase family protein (*deaD*); N-6 DNA methylase (*n6dM*); ATP-dependent zinc metalloprotease (*ftsH*); AAA family ATPase (AAA).

3.4.4. Acetogenesis

The energy-yielding multistep conversion of pyruvate to acetate involves enzyme pyruvate dehydrogenase subunits alpha (Figure 4, PdhA), beta (PdhB), dihydrolipoamide acetyltransferase (PdhC), dihydrolipoamide dehydrogenase (PdhD), and acetate kinase (AckA), of which orthologs are limited to RS, CH, and Hebei-2018 [29,31]. The enzyme involved in the conversion of acetyl-CoA to acetyl phosphate, phosphotrans-acetylase (PtA), is encoded in all four studied genomes. Thus, '*Ca.* P. ziziphi' Jwb-nky is predicted to only partially encode enzymes that are involved in this pathway [30].

Regarding the genomic context of the acetogenesis cluster (Figure 7) of 16SrV phytoplasmas encoding the full cluster, the genes *ackA*, *pdhA/B/C/D*, *thyA* (thymidylate synthase), *tatD* (DNAse family protein), *ligA* (DNA ligase A), and *acpS* show conserved synteny. Moreover, for the acetogenesis cluster, *ftsH*, which is associated with PMUs, was identified in close proximity. Therefore, the acetogenesis cluster of 16SrV phytoplasma might be subject to genomic reductions in '*Ca.* P. ziziphi' Jwb-nky. Genome plasticity between closely related strains is described [21] and also observed within the two '*Ca.* P. ziziphi' strains. However, a loss of glycolysis as the ATP-delivering path increases the impact of carboxylic acid metabolism.

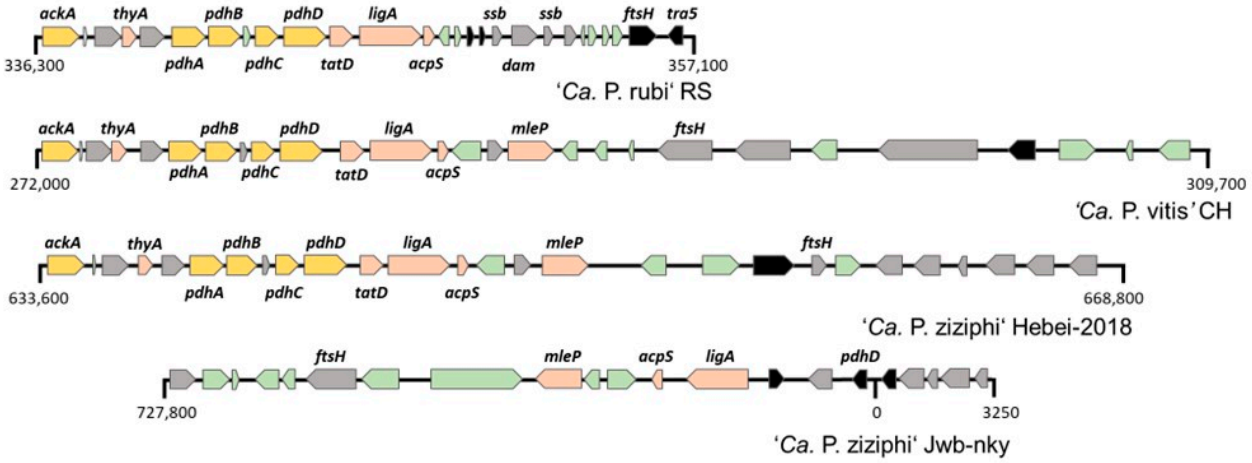

Figure 7. Genomic context of the acetogenesis cluster for 16SrV phytoplasma strains. Gene-encoding proteins involved in pyruvate degradation (yellow), genes with conserved synteny (light red), other genes (grey), hypothetical genes (green), and pseudogenes (black) are indicated with their orientation in the respective chromosome (arrow). Gene names, if displayed, are indicated above the respective location. Genome positions are indicated for each region with respect to the circular organisation of the chromosomes. Gene abbreviations: Acetate kinase (*ackA*); thymidylate synthase (*thyA*); pyruvate dehydrogenase alpha subunit (*pdhA*); pyruvate dehydrogenase beta subunit (*pdhB*); pyruvate dehydrogenase E2 component (*pdhC*); dihydrolipoamide dehydrogenase (*pdhD*); DNase family protein (*tatD*); DNA ligase A (*ligA*), holo-[acyl-carrier protein] synthase (*acpS*); malate: Na^+ Symporter (*mleP*), single-stranded DNA protein (*ssb*); DNA-methylase (*dam*); Zn protease (*ftsH*); transposase (*tra5*).

3.4.5. Glycerophospholipid Metabolism

The enzymes involved in the conversion of dihydroxyacetone phosphate to phosphatidylethanolamine (Figure 4), glycerol-3-phosphate dehydrogenase (GpsA), acyl phosphate glycerol-3-phosphate acyltransferase (PlsY), 1-acyl-sn-glycerol-3-phosphate acyltransferase (PlsC), phosphatidate cytidylyltransferase (CdsA), phosphatidylserinetransferase (PssA), and phosphatidylserine decarboxylase (PsD) are encoded in all four studied genomes. In addition, the genome sequences examined encode the enzyme Holo-acyl-carrier-protein-synthase (AcpS), which mediates the conversion of apo acyl-carrier protein (apo-ACP) to holo-acyl carrier protein (Holo-ACP). In addition, the encoded enzyme phosphate acyltransferase (PlsX) uses Holo-ACP as a substrate to form acyl-phosphate, which is then converted by the previously described PlsY.

Orthologous sequences that code for CDP-diacylglycerol-glycerol-3-phosphate 3-phosphatidyltransferase (PgsA), which catalyses the conversion of glycerol-3-phosphate to phosphatidylglycerophosphate, were only found in the genome sequences of RS, CH, and Hebei-2018 strains.

3.4.6. Glycerol Degradation

Glycerol degradation is mediated by the glycerol dehydrogenase enzyme and dihydroxyacetone kinase with subunits K (DhaK), L, and M, whereby only orthologs for subunit K could be observed. The predicted function of DhaK is the binding of the dihydroxyacetone (dha) substrate, and further catalysation steps are performed by the other subunits [69]. One may speculate that DhaK might facilitate interactions between dha and dihydroxyacetone phosphate (dhap); thereby, there are further possible processing steps carried out by the previously described GpsA in glycerophospholipid metabolism or TpiA in the energy-yielding part of glycolysis. Due to the lack of DhaM multiphosphoryl proteins that are necessary for the phosphorylation of dha, DhaK alone is not functional or able to fulfil miscellaneous functions.

3.5. Secretion of Effectors

The Sec-dependent secretion pathway as a conserved genomic trait in phytoplasma genomes [70] was observed in all four studied genomes, and SecY/E/A for signal-peptide-mediated secretion, YidC insertase for protein assembly, and additional FtsY and SRP54 for the signal recognition particle mediated secretion of oligopeptides (Figure 4, as stated). Secretion via the *Sec*-dependent pathway is facilitated by oligopeptides containing distinctive sequences, which are so-called signal peptides [71], and secretion can be predicted, thereby narrowing down the selection of putative effector proteins to proteins containing signal peptides. Altogether, five different secreted proteins encoded in phytoplasma genomes that are experimentally verified as effectors are described. Oligopeptides, when secreted via the *Sec*-dependent pathway, are putative, host-manipulating effectors [72,73], manipulating host cells with the aim to promote bacterial colonization [74], e.g., by attracting vectors [73]. Herein, TENGU is an oligopeptide that is specific for 16SrI phytoplasmas and induces proliferation in plants via unspecified auxin regulation [75]. Proliferation is as well observed with the secreted SAP05 protein, which additionally induces abnormal leaf growth [76]. The phyllogen protein SAP54 induces phyllody symptoms by degrading floral proteins, resulting in leaf-like flowers [72,77,78]. A homolog of SAP54 was determined in the chromosome of '*Ca.* P. rubi' RS and the two '*Ca.* P. ziziphi' strains (Table S1), thereby suggesting that this protein facilitates the phyllody symptoms observed in host plants. It is proposed that the mode of action of these effectors requires N-terminal coil domains similar to the described SAP54 homolog Zaofeng3 [79], which are shared in the homologs of Hebei-2018, Jwb-nky, and RS. Phyllody symptoms are not observed for the flavescence dorée disease in grapevines, which is consistent with SAP54 not identified for the CH strain. A similar pattern is observed for the described SAP11 homologs SJP1 and SJP2 (Table S1), which are described in '*Ca.* P. ziziphi' [80]. These effector proteins can be found in RS and both '*Ca.* P. ziziphi' strains, and their presence is lacking in the CH strain. SAP11 effectors facilitate proliferation [73] and the formation of witches' broom disease, which is only observed in the host plants of SAP11 homologs containing phytoplasmas of the 16SrV group. The mode of action of SJP1 and SJP2 is based on binding to transcription factors enabled by coiled domains [80], which are predicted for SJP2 in Hebei-2018, Jwb-nky, and RS. SAP54 and SAP11 homologs are three of a total of nine shared proteins containing a signal peptide between '*Ca.* P. ziziphi' strains and '*Ca.* P. rubi' RS (Figure 8). In total, 33 proteins with a signal peptide were predicted for '*Ca.* P. rubi', 23 were predicted for '*Ca.* P. ziziphi' Jwb-nky, 27 were predicted for '*Ca.* P. ziziphi' Hebei-2018, and 12 were predicted for the '*Ca.* P. vitis' CH strain. A total of 95 secreted proteins were predicted in the 16SrV genomes examined, of which only four are conserved (Figure 8). The high number of uniquely predicted secreted proteins (19) that were not assigned to any orthogroup was particularly striking for strain RS (Table S2). These CDS encode hypothetical proteins (17), some of which contain a sequence variable mosaic (SVM) domain (8). It is noteworthy that 8 proteins contain an SVM and a signal peptide, making them interesting candidates for future effector protein studies.

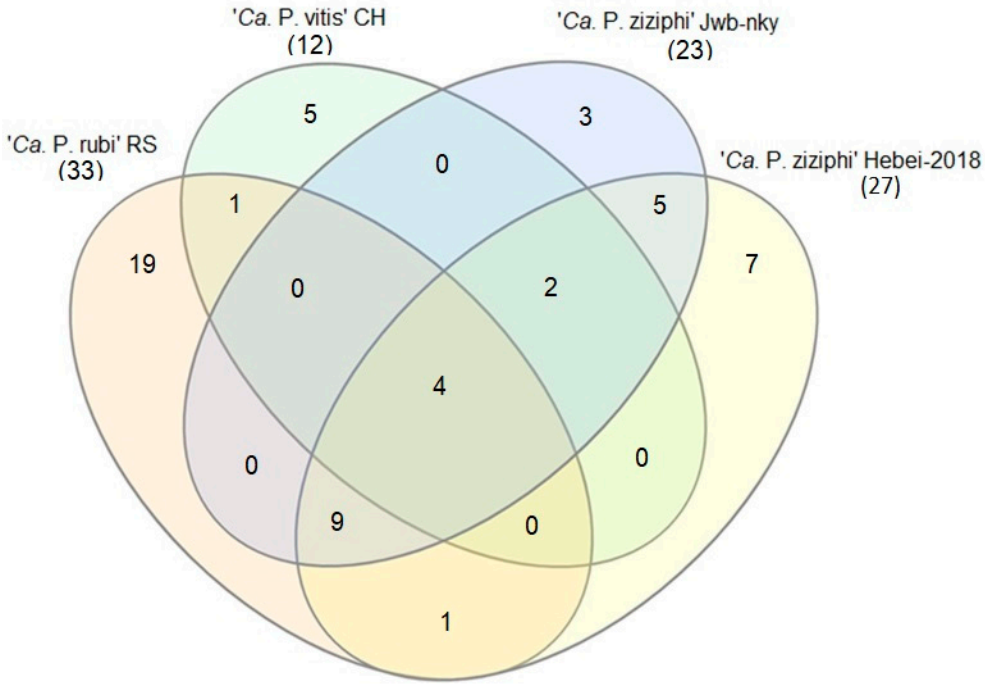

Figure 8. Shared coding sequences with the predicted signal peptide of '*Ca.* P. rubi' RS (orange), '*Ca.* P. vitis' CH (green), '*Ca.* P. ziziphi' Jwb-nky (blue), and '*Ca.* P. ziziphi' Hebei-2018 (yellow). Comparisons with respect to shared or unique characteristics between all three strains and among each other and the amount of unique and shared genomic content are displayed in the Venn diagram. The total CDS number containing a signal peptide of each genome is displayed in brackets.

3.6. Immunodominant Membrane Proteins

Transmission by phloem-sap-sucking vectors is assumed to be the most important means of disease spread for 16SrV phytoplasmas and phytoplasmas in general [1]. During the transmission and colonisation of insects or plants, cell adhesion is an obstacle for phytoplasmas that is overcome by membrane proteins [81,82]. Proteins involved in cell adhesion and that are predicted for '*Ca.* P. rubi' RS, '*Ca.* P. vitis' CH, and '*Ca.* P. ziziphi' Jwb-nky and Hebei-2018 are the insect-associated immunodominant membrane protein (Figure 4, IMP) and variable membrane proteins A and B (VmpA and VmpB). VmpA and B are the orthologs of Vmp1 encoded in '*Ca.* P. solani' [83] and facilitate adhesion to insect membranes in salivary glands and the gut, whereas IMP is associated with membrane adhesion in insects and plants [84,85]. The antigenic membrane protein was not predicted in the 16SrV, supporting the hypothesis that this protein is specific to 16SrI [86]. Immunodominant membrane proteins encoded in 16SrV phytoplasma are conserved in all studied genomes and highly influence pathogen–host interactions via cell adhesion in hosts.

3.7. Whole-Genome Comparison

The current published and complete phytoplasma chromosome sequences consist of 20 genomes, and they were subject to average nucleotide identity (ANI) analysis, resulting in a cluster of 16S ribosomal groups (Figure 9). Tree topology is in accordance with the topology of the phylogenetic tree with 89 marker genes [87]. Two main clusters are formed and consist of 16SrV and 16SrI phytoplasmas. Within the 16SrV group, two subclusters are displayed with the species of '*Ca.* P. ziziphi' in one cluster and CH and RS strains in another cluster, displaying closer relationships at the full-genome level, which were also observed in the phylogenetic analysis of 16S rDNA [7].

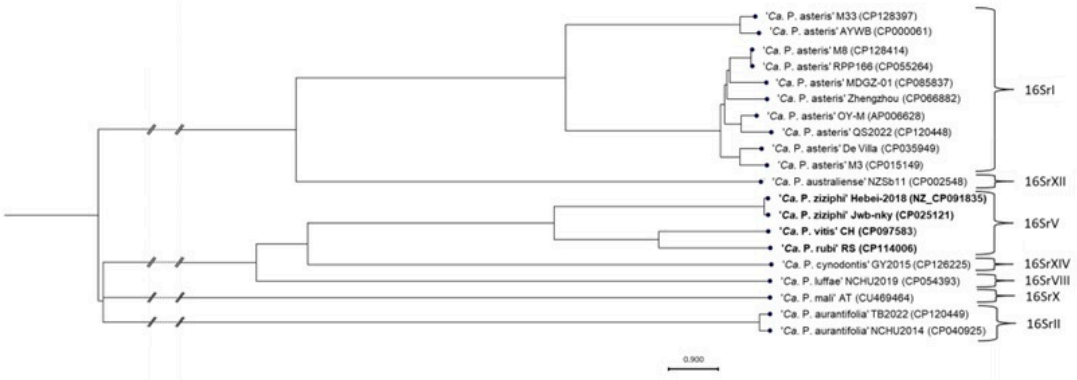

Figure 9. Phylogenetic tree constructed using the neighbour-joining method based on average nucleotide identity comparisons of complete phytoplasma chromosomes. The 16S ribosomal groups are indicated, and 16SrV phytoplasmas are highlighted in bold. The tree is derived to scale with the scale bar indicating 0.9 nucleotide changes.

4. Conclusions

The results of this study highlight the genomic features of the recently published full-genome sequence of '*Ca.* P. rubi' RS in comparison to other 16SrV phytoplasmas. It was demonstrated that the metabolism of *elm yellows phytoplasmas* is distinctive compared to other ribosomal groups via the usage of carboxylic acids. Moreover, the phylogeny of lactate dehydrogenase displays a distinctive cluster of 16SrV phytoplasmas within *Acholeplasmataceae*. Key metabolic features and transporters were shown to be conserved in 16SrV phytoplasmas, with exceptions associated with mobilome elements. The previously described effector repertoire was demonstrated to be conserved in RS, Jwb-nky, and Hebei-2018 strains but not in CH, whereas immunodominant membrane proteins are conserved in all studied genomes. Based on two phylogenetic analyses, it was proven that the studied 16SrV phytoplasmas have a monophyletic relationship, and RS and CH were more closely related than the '*Ca.* P. ziziphi' strains. These results reveal genomic features that are conserved and unique to the 16SrV group, allowing further investigation into the evolutionary origin of phytoplasmas.

Supplementary Materials: The following supporting information can be downloaded at: https://www.mdpi.com/article/10.3390/applmicrobiol3030075/s1. Table S1: Overview of annotated genes with the respective product, pathway, and locus tags for '*Ca.* P. rubi' RS and orthologs in '*Ca.* P. vitis' CH and '*Ca.* P. zizphi' strains, Table S2: Overview of products with predicted signal peptide and corresponding locus tag for '*Ca.* P. rubi' RS, '*Ca.* P. vitis' CH and '*Ca.* P. ziziphi' strains. Products without assigned orthogroup are unique to the respective strain.

Author Contributions: Conceptualization, J.W.B. and M.K.; methodology, J.W.B. and M.K.; software, J.W.B. and D.D.; validation, J.W.B. and M.K.; formal analysis, J.W.B.; investigation, J.W.B.; resources, B.S. and M.K.; data curation, J.W.B., D.D. and M.K.; writing—original draft preparation, J.W.B. and M.K.; writing—review and editing, J.W.B., D.D., B.D., B.S. and M.K.; visualization, J.W.B. and M.K.; supervision, M.K.; project administration, M.K.; funding acquisition, M.K. All authors have read and agreed to the published version of the manuscript.

Funding: This research received no external funding.

Institutional Review Board Statement: Not applicable.

Informed Consent Statement: Not applicable.

Data Availability Statement: Updated annotation for '*Ca.* P. rubi' RS was deposited in GenBank database under accession number CP114006.1.

Conflicts of Interest: The authors declare no conflict of interest.

References

1. Weintraub, P.G.; Beanland, L. Insect vectors of phytoplasmas. *Annu. Rev. Entomol.* **2006**, *51*, 91–111. [CrossRef] [PubMed]
2. IRPCM. '*Candidatus* Phytoplasma', a taxon for the wall-less, non-helical prokaryotes that colonize plant phloem and insects. *Int. J. Syst. Evol. Microbiol.* **2004**, *54*, 1243–1255. [CrossRef]
3. Bertaccini, A.; Arocha-Rosete, Y.; Contaldo, N.; Duduk, B.; Fiore, N.; Montano, H.G.; Kube, M.; Kuo, C.-H.; Martini, M.; Oshima, K.; et al. Revision of the '*Candidatus* Phytoplasma' species description guidelines. *Int. J. Syst. Evol. Microbiol.* **2022**, *72*, 5353. [CrossRef] [PubMed]
4. Lee, I.-M.; Gundersen-Rindal, D.E.; Davis, R.E.; Bartoszyk, I.M. Revised Classification Scheme of Phytoplasmas based on RFLP Analyses of 16S rRNA and Ribosomal Protein Gene Sequences. *Int. J. Syst. Bacteriol.* **1998**, *48*, 1153–1169. [CrossRef]
5. Bertaccini, A.; Lee, I.-M. Phytoplasmas: An Update. In *Characterisation and Epidemiology of Phytoplasma-Associated Diseases*; Rao, G.P., Bertaccini, A., Fiore, N., Liefting, L.W., Eds.; Springer: Singapore, 2018; pp. 1–29. ISBN 978-981-13-0118-6.
6. Lee, I.-M.; Martini, M.; Marcone, C.; Zhu, S.F. Classification of phytoplasma strains in the elm yellows group (16SrV) and proposal of '*Candidatus* Phytoplasma ulmi' for the phytoplasma associated with elm yellows. *Int. J. Syst. Evol. Microbiol.* **2004**, *54*, 337–347. [CrossRef]
7. Malembic-Maher, S.; Salar, P.; Filippin, L.; Carle, P.; Angelini, E.; Foissac, X. Genetic diversity of European phytoplasmas of the 16SrV taxonomic group and proposal of '*Candidatus* Phytoplasma rubi'. *Int. J. Syst. Evol. Microbiol.* **2011**, *61*, 2129–2134. [CrossRef]
8. Khan, M.S.; Raj, S.K.; Snehi, S.K. Natural occurrence of '*Candidatus* Phytoplasma ziziphi' isolates in two species of jujube trees (*Ziziphus* spp.) in India. *Plant Pathol.* **2008**, *57*, 1173. [CrossRef]
9. Caudwell, A.; Gianotti, J.; Kuszala, C.; Larrue, J. Etude du role de particules de type "Mycoplasme" dans l'e'tiologie de la Flavescence dore´e de la vigne. Examen cytologique des plantes malades et des cicadelles infectieuses. *Ann. Phytopathol.* **1971**, *3*, 107–123.
10. Franova, J.; Pribylova, J.; Zemek, R.; Tan, J.L.; Hamborg, Z.; Blystad, D.-R.; Lenz, O.; Koloniuk, I. First report of '*Candidatus* Phytoplasma rubi' associated with *Rubus* stunt disease of raspberry and blackberry in the Czech Republic. *Plant Dis.* **2023**, *107*, 2510. [CrossRef]
11. De Jonghe, K.; Goedefroit, T. First report of '*Candidatus* Phytoplasma rubi' on blackberry in Belgium. *New Dis. Rep.* **2019**, *39*, 19. [CrossRef]
12. Mäurer, R.; Seemüller, E. Nature and genetic relatedness of the mycoplasma-like organism causing *Rubus* stunt in Europe. *Plant Pathol.* **1994**, *44*, 244–249. [CrossRef]
13. Linck, H.; Reineke, A. *Rubus* stunt: A review of an important phytoplasma disease in *Rubus* spp. *J. Plant Dis. Prot.* **2019**, *126*, 393–399. [CrossRef]
14. Chuche, J.; Thiéry, D. Biology and ecology of the Flavescence dorée vector *Scaphoideus titanus*: A review. *Agron. Sustain. Dev.* **2014**, *34*, 381–403. [CrossRef]
15. Schneider, B.; Kätzel, R.; Kube, M. Widespread occurrence of '*Candidatus* Phytoplasma ulmi' in elm species in Germany. *BMC Microbiol.* **2020**, *20*, 74. [CrossRef]
16. Jung, H.-Y.; Sawayanagi, T.; Kakizawa, S.; Nishigawa, H.; Wei, W.; Oshima, K.; Miyata, S.; Ugaki, M.; Hibi, T.; Namba, S. '*Candidatus* phytoplasma ziziphi', a novel phytoplasma taxon associated with jujube witches'-broom disease. *Int. J. Syst. Evol. Microbiol.* **2003**, *53*, 1037–1041. [CrossRef] [PubMed]
17. Holz, S.; Duduk, B.; Büttner, C.; Kube, M. Genetic variability of Alder yellows phytoplasma in *Alnus glutinosa* in its natural Spreewald habitat. *For. Path.* **2016**, *46*, 11–21. [CrossRef]
18. Wei, W.; Zhao, Y. Phytoplasma Taxonomy: Nomenclature, Classification, and Identification. *Biology* **2022**, *11*, 1119. [CrossRef]
19. Christensen, N.M.; Axelsen, K.B.; Nicolaisen, M.; Schulz, A. Phytoplasmas and their interactions with hosts. *Trends Plant Sci.* **2005**, *10*, 526–535. [CrossRef]
20. Kube, M.; Mitrovic, J.; Duduk, B.; Rabus, R.; Seemüller, E. Current view on phytoplasma genomes and encoded metabolism. *Sci. World J.* **2012**, *2012*, 185942. [CrossRef]
21. Andersen, M.T.; Liefting, L.W.; Havukkala, I.; Beever, R.E. Comparison of the complete genome sequence of two closely related isolates of '*Candidatus* Phytoplasma australiense' reveals genome plasticity. *BMC Genom.* **2013**, *14*, 529. [CrossRef]
22. Marcone, C.; Schneider, B.; Seemüller, E. '*Candidatus* Phytoplasma cynodontis', the phytoplasma associated with Bermuda grass white leaf disease. *Int. J. Syst. Evol. Microbiol.* **2004**, *54*, 1077–1082. [CrossRef] [PubMed]
23. Kube, M.; Siewert, C.; Migdoll, A.M.; Duduk, B.; Holz, S.; Rabus, R.; Seemüller, E.; Mitrovic, J.; Müller, I.; Büttner, C.; et al. Analysis of the complete genomes of *Acholeplasma brassicae*, *A. palmae* and *A. laidlawii* and their comparison to the obligate parasites from '*Candidatus* Phytoplasma'. *J. Mol. Microbiol. Biotechnol.* **2014**, *24*, 19–36. [CrossRef] [PubMed]
24. Oshima, K.; Kakizawa, S.; Nishigawa, H.; Jung, H.-Y.; Wei, W.; Suzuki, S.; Arashida, R.; Nakata, D.; Miyata, S.; Ugaki, M.; et al. Reductive evolution suggested from the complete genome sequence of a plant-pathogenic phytoplasma. *Nat. Genet.* **2004**, *36*, 27–29. [CrossRef]
25. Silva, Z.; Sampaio, M.-M.; Henne, A.; Böhm, A.; Gutzat, R.; Boos, W.; da Costa, M.S.; Santos, H. The high-affinity maltose/trehalose ABC transporter in the extremely thermophilic bacterium *Thermus thermophilus* HB27 also recognizes sucrose and palatinose. *J. Bacteriol.* **2005**, *187*, 1210–1218. [CrossRef] [PubMed]

26. Oshima, K.; Ishii, Y.; Kakizawa, S.; Sugawara, K.; Neriya, Y.; Himeno, M.; Minato, N.; Miura, C.; Shiraishi, T.; Yamaji, Y.; et al. Dramatic transcriptional changes in an intracellular parasite enable host switching between plant and insect. *PLoS ONE* **2011**, *6*, e23242. [CrossRef]
27. Sobczak, I.; Lolkema, J.S. The 2-hydroxycarboxylate transporter family: Physiology, structure, and mechanism. *Microbiol. Mol. Biol. Rev.* **2005**, *69*, 665–695. [CrossRef]
28. Kube, M.; Schneider, B.; Kuhl, H.; Dandekar, T.; Heitmann, K.; Migdoll, A.M.; Reinhardt, R.; Seemüller, E. The linear chromosome of the plant-pathogenic mycoplasma '*Candidatus* Phytoplasma mali'. *BMC Genom.* **2008**, *9*, 306. [CrossRef]
29. Debonneville, C.; Mandelli, L.; Brodard, J.; Groux, R.; Roquis, D.; Schumpp, O. The Complete Genome of the "Flavescence Dorée" Phytoplasma Reveals Characteristics of Low Genome Plasticity. *Biology* **2022**, *11*, 953. [CrossRef]
30. Wang, J.; Song, L.; Jiao, Q.; Yang, S.; Gao, R.; Lu, X.; Zhou, G. Comparative genome analysis of jujube witches'-broom Phytoplasma, an obligate pathogen that causes jujube witches'-broom disease. *BMC Genom.* **2018**, *19*, 689. [CrossRef]
31. Xue, C.; Zhang, Y.; Li, H.; Liu, Z.; Gao, W.; Liu, M.; Wang, H.; Liu, P.; Zhao, J. The genome of *Candidatus* phytoplasma ziziphi provides insights into their biological characteristics. *BMC Plant Biol.* **2023**, *23*, 251. [CrossRef]
32. Duckeck, D.; Zübert, C.; Böhm, J.W.; Carminati, G.; Schneider, B.; Kube, M. Complete Genome of "*Candidatus* Phytoplasma rubi" RS, a Phytopathogenic Bacterium Associated with *Rubus* Stunt Disease. *Microbiol. Resour. Announc.* **2023**, *12*, e0130322. [CrossRef] [PubMed]
33. Rutherford, K.; Parkhill, J.; Crook, J.; Horsnell, T.; Rice, P.; Rajandream, M.A.; Barrell, B. Artemis: Sequence visualization and annotation. *Bioinformatics* **2000**, *16*, 944–945. [CrossRef] [PubMed]
34. Aziz, R.K.; Bartels, D.; Best, A.A.; DeJongh, M.; Disz, T.; Edwards, R.A.; Formsma, K.; Gerdes, S.; Glass, E.M.; Kubal, M.; et al. The RAST Server: Rapid annotations using subsystems technology. *BMC Genom.* **2008**, *9*, 75. [CrossRef]
35. Altschul, S.F.; Gish, W.; Miller, W.; Myers, E.W.; Lipman, D.J. Basic local alignment search tool. *J. Mol. Biol.* **1990**, *215*, 403–410. [CrossRef]
36. Sayers, E.W.; Bolton, E.E.; Brister, J.R.; Canese, K.; Chan, J.; Comeau, D.C.; Connor, R.; Funk, K.; Kelly, C.; Kim, S.; et al. Database resources of the national center for biotechnology information. *Nucleic Acids Res.* **2022**, *50*, D20–D26. [CrossRef] [PubMed]
37. Caspi, R.; Altman, T.; Billington, R.; Dreher, K.; Foerster, H.; Fulcher, C.A.; Holland, T.A.; Keseler, I.M.; Kothari, A.; Kubo, A.; et al. The MetaCyc database of metabolic pathways and enzymes and the BioCyc collection of Pathway/Genome Databases. *Nucleic Acids Res.* **2014**, *42*, D459–D471.
38. Kaneshisa, M.; Goto, S. Kyoto Encyclopedia of Genes and Genomes. *Nucleic Acids Res.* **2000**, *28*, 27–30. [CrossRef] [PubMed]
39. Jones, P.; Binns, D.; Chang, H.-Y.; Fraser, M.; Li, W.; McAnulla, C.; McWilliam, H.; Maslen, J.; Mitchell, A.; Nuka, G.; et al. InterProScan 5: Genome-scale protein function classification. *Bioinformatics* **2014**, *30*, 1236–1240. [CrossRef]
40. Käll, L.; Krogh, A.; Sonnhammer, E.L.L. A combined transmembrane topology and signal peptide prediction method. *J. Mol. Biol.* **2004**, *338*, 1027–1036. [CrossRef]
41. Altenhoff, A.M.; Train, C.-M.; Gilbert, K.J.; Mediratta, I.; Mendes de Farias, T.; Moi, D.; Nevers, Y.; Radoykova, H.-S.; Rossier, V.; Warwick Vesztrocy, A.; et al. OMA orthology in 2021: Website overhaul, conserved isoforms, ancestral gene order and more. *Nucleic Acids Res.* **2021**, *49*, D373–D379. [CrossRef]
42. Emms, D.M.; Kelly, S. OrthoFinder2: Fast and accurate phylogenomic orthology analysis from gene sequences. *Genome Biol.* **2018**, *20*, 238. [CrossRef]
43. Heberle, H.; Meirelles, G.V.; Da Silva, F.R.; Telles, G.P.; Minghim, R. InteractiVenn: A web-based tool for the analysis of sets through Venn diagrams. *BMC Bioinform.* **2015**, *16*, 169.
44. Tamura, K.; Stecher, G.; Kumar, S. MEGA11: Molecular Evolutionary Genetics Analysis Version 11. *Mol. Biol. Evol.* **2021**, *38*, 3022–3027. [CrossRef]
45. Bai, X.; Zhang, J.; Ewing, A.; Miller, S.A.; Jancso Radek, A.; Shevchenko, D.V.; Tsukerman, K.; Walunas, T.; Lapidus, A.; Campbell, J.W.; et al. Living with genome instability: The adaptation of phytoplasmas to diverse environments of their insect and plant hosts. *J. Bacteriol.* **2006**, *188*, 3682–3696. [CrossRef]
46. Tokuda, R.; Iwabuchi, N.; Kitazawa, Y.; Nijo, T.; Suzuki, M.; Maejima, K.; Oshima, K.; Namba, S.; Yamaji, Y. Potential mobile units drive the horizontal transfer of phytoplasma effector phyllogen genes. *Front. Genet.* **2023**, *14*, 1132432. [CrossRef]
47. Huang, C.-T.; Cho, S.-T.; Lin, Y.-C.; Tan, C.-M.; Chiu, Y.-C.; Yang, J.-Y.; Kuo, C.-H. Comparative Genome Analysis of '*Candidatus* Phytoplasma luffae' Reveals the Influential Roles of Potential Mobile Units in Phytoplasma Evolution. *Front. Microbiol.* **2022**, *13*, 773608. [CrossRef]
48. Li, Q.; Xu, H.; Zhang, W.; Sun, J.; Yue, Y. Extraction of cucumber phloem sap based on the capillary-air pressure principle. *Biotechniques* **2022**, *72*, 233–243. [CrossRef] [PubMed]
49. Killiny, N.; Hijaz, F.; El-Shesheny, I.; Alfaress, S.; Jones, S.E.; Rogers, M.E. Metabolomic analyses of the haemolymph of the Asian citrus psyllid *Diaphorina citri*, the vector of huanglongbing. *Physiol. Entomol.* **2017**, *42*, 134–145. [CrossRef]
50. van Dongen, J.T.; Schurr, U.; Pfister, M.; Geigenberger, P. Phloem metabolism and function have to cope with low internal oxygen. *Plant Physiol.* **2003**, *131*, 1529–1543. [CrossRef]
51. Weise, S.E.; Weber, A.P.M.; Sharkey, T.D. Maltose is the major form of carbon exported from the chloroplast at night. *Planta* **2004**, *218*, 474–482. [CrossRef]
52. Heitkamp, T.; Kalinowski, R.; Böttcher, B.; Börsch, M.; Altendorf, K.; Greie, J.-C. K+-translocating KdpFABC P-type ATPase from *Escherichia coli* acts as a functional and structural dimer. *Biochemistry* **2008**, *47*, 3564–3575. [CrossRef]

53. Sukharev, S.I.; Blount, P.; Martinac, B.; Blattner, F.R.; Kung, C. A large-conductance mechanosensitive channel in *E. coli* encoded by mscL alone. *Nature* **1994**, *368*, 265–268. [CrossRef] [PubMed]
54. Siewert, C.; Luge, T.; Duduk, B.; Seemüller, E.; Büttner, C.; Sauer, S.; Kube, M. Analysis of expressed genes of the bacterium '*Candidatus* Phytoplasma mali' highlights key features of virulence and metabolism. *PLoS ONE* **2014**, *9*, e94391. [CrossRef]
55. Poolman, B.; Molenaar, D.; Smid, E.J.; Ubbink, T.; Abee, T.; Renault, P.P.; Konings, W.N. Malolactic fermentation: Electrogenic malate uptake and malate/lactate antiport generate metabolic energy. *J. Bacteriol.* **1991**, *173*, 6030–6037. [CrossRef] [PubMed]
56. Béven, L.; Charenton, C.; Dautant, A.; Bouyssou, G.; Labroussaa, F.; Sköllermo, A.; Persson, A.; Blanchard, A.; Sirand-Pugnet, P. Specific evolution of F1-like ATPases in mycoplasmas. *PLoS ONE* **2012**, *7*, e38793. [CrossRef] [PubMed]
57. Russell, R.R.; Aduse-Opoku, J.; Sutcliffe, I.C.; Tao, L.; Ferretti, J.J. A binding protein-dependent transport system in *Streptococcus mutans* responsible for multiple sugar metabolism. *J. Biol. Chem.* **1992**, *267*, 4631–4637. [CrossRef]
58. Franceus, J.; Desmet, T. Sucrose Phosphorylase and Related Enzymes in Glycoside Hydrolase Family 13: Discovery, Application and Engineering. *Int. J. Mol. Sci.* **2020**, *21*, 2526. [CrossRef] [PubMed]
59. Lu, Z.; Dunaway-Mariano, D.; Allen, K.N. HAD superfamily phosphotransferase substrate diversification: Structure and function analysis of HAD subclass IIB sugar phosphatase BT4131. *Biochemistry* **2005**, *44*, 8684–8696. [CrossRef]
60. Chung, W.-C.; Chen, L.-L.; Lo, W.-S.; Lin, C.-P.; Kuo, C.-H. Comparative analysis of the peanut witches'-broom phytoplasma genome reveals horizontal transfer of potential mobile units and effectors. *PLoS ONE* **2013**, *8*, e62770. [CrossRef] [PubMed]
61. Feldman-Salit, A.; Hering, S.; Messiha, H.L.; Veith, N.; Cojocaru, V.; Sieg, A.; Westerhoff, H.V.; Kreikemeyer, B.; Wade, R.C.; Fiedler, T. Regulation of the activity of lactate dehydrogenases from four lactic acid bacteria. *J. Biol. Chem.* **2013**, *288*, 21295–21306. [CrossRef]
62. Cordwell, S.J.; Basseal, D.J.; Pollack, J.D.; Humphery-Smith, I. Malate/lactate dehydrogenase in mollicutes: Evidence for a multienzyme protein. *Gene* **1997**, *195*, 113–120. [CrossRef] [PubMed]
63. Masukagami, Y.; Tivendale, K.A.; Browning, G.F.; Sansom, F.M. Analysis of the *Mycoplasma bovis* lactate dehydrogenase reveals typical enzymatic activity despite the presence of an atypical catalytic site motif. *Microbiology* **2018**, *164*, 186–193. [CrossRef] [PubMed]
64. Neimark, H.; Tung, M.C. Properties of a fructose-1,6-diphosphate-activated lactate dehydrogenase from *Acholeplasma laidlawii* type A. *J. Bacteriol.* **1973**, *114*, 1025–1033. [CrossRef] [PubMed]
65. Loreti, E.; Perata, P. The Many Facets of Hypoxia in Plants. *Plants* **2020**, *9*, 745. [CrossRef]
66. Sears, B.B.; Klomparens, K.L.; Wood, J.I.; Schewe, J.I. Effect of Altered Levels of Oxygen and Carbon Dioxide on Phytoplasma Abundance in *Oenothera* Leaftip Cultures. *Physiol. Mol. Plant Pathol.* **1997**, *50*, 275–287. [CrossRef]
67. Cvrković, T.; Jović, J.; Mitrović, M.; Krstić, O.; Toševski, I. Distribution of alder yellows phytoplasma on common and gray alder (*Alnus glutinosa* and *Alnus incana*) in Serbia. *Zaštita Bilja* **2011**, *62*, 185–196.
68. Wei, W.; Davis, R.E.; Jomantiene, R.; Zhao, Y. Ancient, recurrent phage attacks and recombination shaped dynamic sequence-variable mosaics at the root of phytoplasma genome evolution. *Proc. Natl. Acad. Sci. USA* **2008**, *105*, 11827–11832. [CrossRef]
69. Garcia-Alles, L.F.; Siebold, C.; Nyffeler, T.L.; Flükiger-Brühwiler, K.; Schneider, P.; Bürgi, H.-B.; Baumann, U.; Erni, B. Phosphoenolpyruvate- and ATP-dependent dihydroxyacetone kinases: Covalent substrate-binding and kinetic mechanism. *Biochemistry* **2004**, *43*, 13037–13045. [CrossRef]
70. Oshima, K.; Maejima, K.; Namba, S. Genomic and evolutionary aspects of phytoplasmas. *Front. Microbiol.* **2013**, *4*, 230. [CrossRef] [PubMed]
71. Perlman, D.; Halvorson, H.O. A putative signal peptidase recognition site and sequence in eukaryotic and prokaryotic signal peptides. *J. Mol. Biol.* **1983**, *167*, 391–409. [CrossRef]
72. MacLean, A.M.; Sugio, A.; Makarova, O.V.; Findlay, K.C.; Grieve, V.M.; Tóth, R.; Nicolaisen, M.; Hogenhout, S.A. Phytoplasma effector SAP54 induces indeterminate leaf-like flower development in *Arabidopsis* plants. *Plant Physiol.* **2011**, *157*, 831–841. [CrossRef] [PubMed]
73. Sugio, A.; Kingdom, H.N.; MacLean, A.M.; Grieve, V.M.; Hogenhout, S.A. Phytoplasma protein effector SAP11 enhances insect vector reproduction by manipulating plant development and defense hormone biosynthesis. *Proc. Natl. Acad. Sci. USA* **2011**, *108*, E1254–E1263. [CrossRef] [PubMed]
74. Tseng, T.-T.; Tyler, B.M.; Setubal, J.C. Protein secretion systems in bacterial-host associations, and their description in the Gene Ontology. *BMC Microbiol.* **2009**, *9* (Suppl. 1), S2. [CrossRef] [PubMed]
75. Wang, Q.; Guo, Y.; Wang, N.; Li, Y.; Chen, W.; Chen, W.; Wu, Y. Identification of a Conserved Core Genome with Group-Specific Genes from Comparative Genomics of Ten Different *Candidatus* Phytoplasma Strains. *J. Phytopathol.* **2014**, *162*, 650–659. [CrossRef]
76. Huang, W.; MacLean, A.M.; Sugio, A.; Maqbool, A.; Busscher, M.; Cho, S.-T.; Kamoun, S.; Kuo, C.-H.; Immink, R.G.H.; Hogenhout, S.A. Parasitic modulation of host development by ubiquitin-independent protein degradation. *Cell* **2021**, *184*, 5201–5214.e12. [CrossRef]
77. Hoshi, A.; Oshima, K.; Kakizawa, S.; Ishii, Y.; Ozeki, J.; Hashimoto, M.; Komatsu, K.; Kagiwada, S.; Yamaji, Y.; Namba, S. A unique virulence factor for proliferation and dwarfism in plants identified from a phytopathogenic bacterium. *Proc. Natl. Acad. Sci. USA* **2009**, *106*, 6416–6421. [CrossRef]
78. Kitazawa, Y.; Iwabuchi, N.; Himeno, M.; Sasano, M.; Koinuma, H.; Nijo, T.; Tomomitsu, T.; Yoshida, T.; Okano, Y.; Yoshikawa, N.; et al. Phytoplasma-conserved phyllogen proteins induce phyllody across the Plantae by degrading floral MADS domain proteins. *J. Exp. Bot.* **2017**, *68*, 2799–2811. [CrossRef] [PubMed]

79. Chen, P.; Zhang, Y.; Li, Y.; Yang, Q.; Li, Q.; Chen, L.; Chen, Y.; Ye, X.; Tan, B.; Zheng, X.; et al. Jujube witches' broom phytoplasma effector Zaofeng3, a homologous effector of SAP54, induces abnormal floral organ development and shoot proliferation. *Phytopathology* **2023**. [CrossRef]
80. Zhou, J.; Ma, F.; Yao, Y.; Deng, M.; Chen, M.; Zhang, S.; Li, Y.; Yang, J.; Zhang, N.; Huang, J.; et al. Jujube witches' broom phytoplasma effectors SJP1 and SJP2 induce lateral bud outgrowth by repressing the ZjBRC1-controlled auxin efflux channel. *Plant Cell Environ.* **2021**, *44*, 3257–3272. [CrossRef]
81. Arricau-Bouvery, N.; Duret, S.; Dubrana, M.-P.; Batailler, B.; Desqué, D.; Béven, L.; Danet, J.-L.; Monticone, M.; Bosco, D.; Malembic-Maher, S.; et al. Variable Membrane Protein A of Flavescence Dorée Phytoplasma Binds the Midgut Perimicrovillar Membrane of *Euscelidius variegatus* and Promotes Adhesion to Its Epithelial Cells. *Appl. Environ. Microbiol.* **2018**, *84*, e02487-17. [CrossRef]
82. Konnerth, A.; Krczal, G.; Boonrod, K. Immunodominant membrane proteins of phytoplasmas. *Microbiol. Read.* **2016**, *162*, 1267–1273. [CrossRef] [PubMed]
83. Cimerman, A.; Pacifico, D.; Salar, P.; Marzachì, C.; Foissac, X. Striking diversity of vmp1, a variable gene encoding a putative membrane protein of the stolbur phytoplasma. *Appl. Environ. Microbiol.* **2009**, *75*, 2951–2957. [CrossRef]
84. Trivellone, V.; Ripamonti, M.; Angelini, E.; Filippin, L.; Rossi, M.; Marzachí, C.; Galetto, L. Evidence suggesting interactions between immunodominant membrane protein Imp of Flavescence dorée phytoplasma and protein extracts from distantly related insect species. *J. Appl. Microbiol.* **2019**, *127*, 1801–1813. [CrossRef]
85. Boonrod, K.; Munteanu, B.; Jarausch, B.; Jarausch, W.; Krczal, G. An immunodominant membrane protein (Imp) of '*Candidatus* Phytoplasma mali' binds to plant actin. *Mol. Plant Microbe Interact.* **2012**, *25*, 889–895. [CrossRef]
86. Galetto, L.; Bosco, D.; Balestrini, R.; Genre, A.; Fletcher, J.; Marzachì, C. The major antigenic membrane protein of "*Candidatus* Phytoplasma asteris" selectively interacts with ATP synthase and actin of leafhopper vectors. *PLoS ONE* **2011**, *6*, e22571. [CrossRef] [PubMed]
87. Kirdat, K.; Tiwarekar, B.; Sathe, S.; Yadav, A. From sequences to species: Charting the phytoplasma classification and taxonomy in the era of taxogenomics. *Front. Microbiol.* **2023**, *14*, 1123783. [CrossRef] [PubMed]